

## Critical imperfect nesting in (TMTSF)<sub>2</sub>PF<sub>6</sub>

G. M. Danner\* and P. M. Chaikin

*Department of Physics, Princeton University, Princeton, New Jersey 08544*

S. T. Hannahs

*NHMFL, Florida State University, Tallahassee, Florida 32306*

(Received 24 August 1995)

We have investigated the temperature, pressure, and field dependence of the spin density wave (SDW) transition in the organic superconductor (TMTSF)<sub>2</sub>PF<sub>6</sub> and derived parameters for this transition. The SDW can be characterized by the degree to which the two Fermi surfaces couple or “nest” as measured by the imperfect nesting bandwidth  $t'_b$ . Perfect nesting (maximum  $T_{\text{SDW}}$ ) occurs for  $t'_b=0$ , and increasing pressure increases  $t'_b$  and suppresses  $T_{\text{SDW}}$  to 0 K at a critical value  $t'_b^*$ . The increase of  $T_{\text{SDW}}$  with field has been shown to be orbitally driven, and the field dependence is nearly quadratic for fields in the **c** direction. We have made quantitative observations of the field dependence of  $T_{\text{SDW}}$  at ambient pressure to 29 T and under hydrostatic pressure to 8 T. From our measurements at ambient pressure we are able to extract  $t'_b$  and  $t'_b^*$  using mean field theory and observe  $T_{\text{SDW}}=12.1\pm 0.1$  K,  $t'_b=4.5\pm 0.3$  K, and  $t'_b^*=11.3\pm 0.2$  K. Under a hydrostatic pressure of  $5.2\pm 0.2$  kbar,  $t'_b$  increases to  $11.0\pm 0.3$  K with  $T_{\text{SDW}}$  decreasing to  $3.3\pm 0.1$  K. The high pressure results are consistent with the value of  $t'_b^*$  from the ambient pressure measurements. We also observe no dependence of  $T_{\text{SDW}}$  with field in the **a** or **b** directions, in contrast to previous results.

### I. INTRODUCTION

Peierls<sup>1</sup> predicted that a one-dimensional (1D) metal is unstable in a metal-insulator transition at finite temperature. There would be a charge distortion induced by a potential with wave vector  $2k_F$  which opens up a gap at the Fermi surface. This new state is favored because the energy cost of the charge distortion (and resulting lattice distortion) is less than the energy gain from lowering the energy of the large number of electron states near the Fermi surface by forming a gap.

There is another class of systems with a Peierls-like instability that does not involve a static charge distortion or lattice distortion. In these systems the electrons are exchange coupled, and a spin density wave (SDW) is responsible for opening a gap at the Fermi surface. This is the situation in organic superconductors.

The material under study is a member of the Bechgaard salts and is based on the organic molecule tetramethyltetraselenefulvaline (TMTSF).<sup>2</sup> The compounds (TMTSF)<sub>2</sub>X are highly anisotropic organic conductors with a rich phase diagram exhibiting spin density wave (SDW), metallic, superconducting, and field-induced SDW quantum Hall phases at low temperatures. The transitions between these phases depend on pressure, temperature, magnetic field, and the anion of the salt (labeled X above). We will be concentrating on the SDW phase, which occurs at  $\sim 12$  K at ambient pressure and zero field in (TMTSF)<sub>2</sub>PF<sub>6</sub> (hereafter PF<sub>6</sub>). The SDW transition temperature can be suppressed by pressure and is below the superconducting transition temperature ( $\sim 1$  K) at  $\sim 6$  kbar. The crystal has highly conducting chains along the **a** direction which are responsible for the 1D properties. These chains couple in the **b** direction to form conducting planes with the weakest coupling being perpendicular to the planes along the **c** direction. The bandwidths along the crys-

tal axes are  $4t_a:4t_b:4t_c \approx 1$  eV: 0.1 eV: 0.003 eV, and the Fermi surfaces consist of slightly warped parallel sheets at  $k_x \sim \pm k_F$ .

### II. NESTING AND IMPERFECT NESTING

In a truly 1D system fluctuations prevent the transition from occurring except at  $T=0$  K. In real materials with 1D character, the albeit small interaction between 1D chains stabilizes the phase transition and endows it with a nonzero transition temperature. However, in a 2D system it is most common to have band structures where large numbers of states cannot be coupled by a single wave vector. The energy gain from coupling a small number of states is not sufficient to allow the SDW state to occur.

In the  $k_z=0$  plane, the band structure of the Bechgaard salts is well described by<sup>3,4</sup>

$$E(\vec{k}) = -2t_a \cos(k_x a), -2t_b \cos(k_y b), \quad (1)$$

or

$$E(\vec{k}) = \hbar v_F (|k_x| - k_F) - 2t_b \cos(k_y b) - 2t'_b \cos(2k_y b). \quad (2)$$

This produces a quasi-one-dimensional Fermi surface consisting of warped sheets centered at  $k_x \sim \pm k_F$ . In this case a potential with wave vector  $\vec{Q}=(2k_F, 0)$  (in analogy to the 1D case) would only couple a few states at the Fermi surface. It has been shown<sup>5</sup> that for a system with tetragonal symmetry, the optimal distortion vector is  $\vec{Q}=(2k_F, \pi/b, \pi/b)$ . This wave vector couples (or “nests”) nearly all of the states on one Fermi sheet into the other. This is shown in Fig. 1 for two dimensions where the nesting vector is  $\vec{Q}=(2k_F, \pi/b)$ . In fact the actual nesting vector is incom-

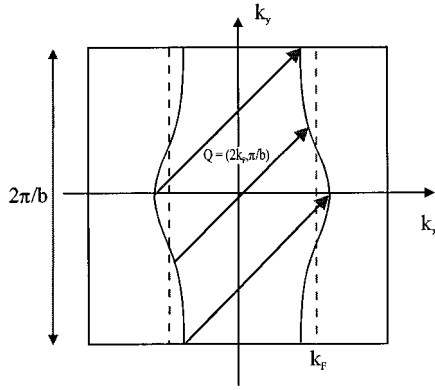


FIG. 1. Band structure in a quasi-1D metal showing the nesting vector  $\vec{Q} = (2k_F, 2\pi/b)$ . If  $t'_b = 0$  in Eq. (2), then this vector would couple all of the states on the Fermi surface.

mensurate and has been measured as  $\vec{Q} = (\frac{1}{2}, \frac{1}{4} + \delta, 0)$  in  $\text{PF}_6$  (Ref. 6) using the unit cell in real space, which has a triclinic symmetry.

The nesting of the Fermi surfaces described by Eq. (1) is not perfect because it does not couple all the states at the Fermi surface. As the magnitude of the transfer integral in the  $\mathbf{b}$  direction becomes larger (i.e., the system is closer to 2D) the SDW phase will be suppressed to lower temperature and eventually suppressed completely.<sup>3</sup> We will use the band structure form in Eq. (2), which has been linearized around the Fermi surface, for the subsequent discussion. In this form the term  $t'_b$  is called the imperfect nesting bandwidth. If  $t'_b = 0$ , then there is a single wave vector that *will* nest the entire Fermi surface, and  $t'_b \neq 0$  will leave parts of the Fermi surface *unnested*. The suppression of the critical temperature with the degree of imperfect nesting ( $t'_b$ ) can be calculated,<sup>4</sup> and by varying the pressure on the sample one can experimentally vary  $t'_b$  and (to a lesser extent)  $t_b$ . Within this same framework one can predict the dependence of the transition temperature on magnetic field and  $t'_b$  with the result

$$T_c(H) = T_c(0) + f(\beta) \frac{\omega_c^2}{t_b'^*}. \quad (3)$$

Here  $f(\beta)$  is a dimensionless function of the ratio ( $\beta$ ) of the imperfect nesting ( $t'_b$ ) to the value of imperfect nesting sufficient to destroy the SDW ( $t_b'^*$ ). The term  $\omega_c = e v_F b H / 2$  is the frequency that the electron traverses the first Brillouin zone on its open orbit trajectory in the  $\mathbf{b}$  direction with a field in the  $\mathbf{c}$  direction ( $\omega_c / H \sim 0.89$  K/T for  $\text{PF}_6$ ).

### III. EXPERIMENT

The measurements were performed on single-crystal samples of  $\text{PF}_6$  grown in our laboratory.<sup>7</sup> Contacts were made to the samples using 0.001 in. Au wire and silver paint, and four-probe resistance measurements were made using conventional low-frequency lock-in amplifier techniques. For measurements of the highly conducting  $\mathbf{a}$  axis, two current leads were attached at the ends of the sample which were covered by silver paint to ensure uniform current distribution. Two voltage leads were attached along each side of the sample to measure  $R_{xx}$  and  $R_{xy}$ . Measurements of the

least conducting  $\mathbf{c}$  axis used pairs of contacts placed on the top and bottom  $\mathbf{ab}$  planes. Currents were adjusted to ensure that the resistance was linear in the current. For the high-pressure measurements, the samples were attached to a high-pressure feedthrough.<sup>8</sup> The beryllium-copper pressure clamps were 0.5 in. diam  $\times$  1.5 in. long, and are capable of hydrostatic pressures from 0 to 18 kbar. Ambient pressure measurements were made using a probe with a gear driven “flipper” stage that could be rotated  $360^\circ +$  perpendicular to the probe’s long axis. In this way the samples could be aligned in field along two of the three crystal axes to within a few degrees. Magnetic fields were created using two different sources. For fields up to 9 T, we used a split-coil superconducting magnet in which we could precisely adjust the angle of the field with respect to the sample using a goniometer. This was the magnet used for the high-pressure measurements. Fields to 30 T were achieved at the Francis Bitter National Magnet Laboratory in the Hybrid II magnet. This was used for the ambient pressure measurements. Temperatures were measured using a capacitor and capacitance bridge calibrated in zero field.

The pressures were measured by observing the suppression in the superconducting transition temperature in high-purity lead.<sup>9</sup> Small coils with lead inside were placed inside and outside the cell. The mutual inductance between each of these coils and a drive coil was observed to measure the transition temperature of the lead. Using two coils eliminates many systematic errors associated with temperature calibrations and allows a pressure resolution of  $\sim 0.1$  kbar.

## IV. MEASUREMENTS OF $T_{\text{SDW}}(\vec{H}, P)$

### A. Ambient pressure

Measurements have been made of  $R_{xx}$  in the region of the SDW transition in  $\text{PF}_6$  at ambient pressure. In zero field we measure the gap from the Arrhenius form of the temperature dependence of the resistance with the result that  $\Delta = 14\text{--}23$  K. Other measurements were conducted in fields to 29 T, and separate observations were made with the field oriented along the three primary crystal axes. There were two samples on the “flipper” probe such that a  $\mathbf{b}$  and  $\mathbf{c}$  axis orientation or a  $\mathbf{c}$  and  $\mathbf{a}$  axis orientation could be measured simultaneously. This provided a check on the uniformity of the temperature sweeps. The crystals were aligned by hand at room temperature, and the  $\mathbf{bc}$  plane or  $\mathbf{ac}$  plane was aligned to within a few degrees. Two sets of samples were measured which gave similar results, but only the data for the second set are presented here. Measurements of the resistive transition with the field oriented along  $\mathbf{a}$  and  $\mathbf{b}$  are shown in Figs. 2 and 3. In both cases there is a steep rise in the resistance at the transition temperature, and the resistance changes by nearly an order of magnitude between 8 and 16 K. Also there is only a small amount of magnetoresistance when the field is in the conducting plane both above and below  $T_{\text{SDW}}$ . The transition temperature can be more precisely determined by taking the derivative of the logarithm of the resistance vs  $1/T$ . If the resistance is of a simple Arrhenius form, this will allow one to extract the gap energy. There is also a peak in the derivative at the transition temperature. We see from these plots that there is no field dependence to the transition temperature when the field is in the  $\mathbf{a}$  or  $\mathbf{b}$  directions. This result contra-

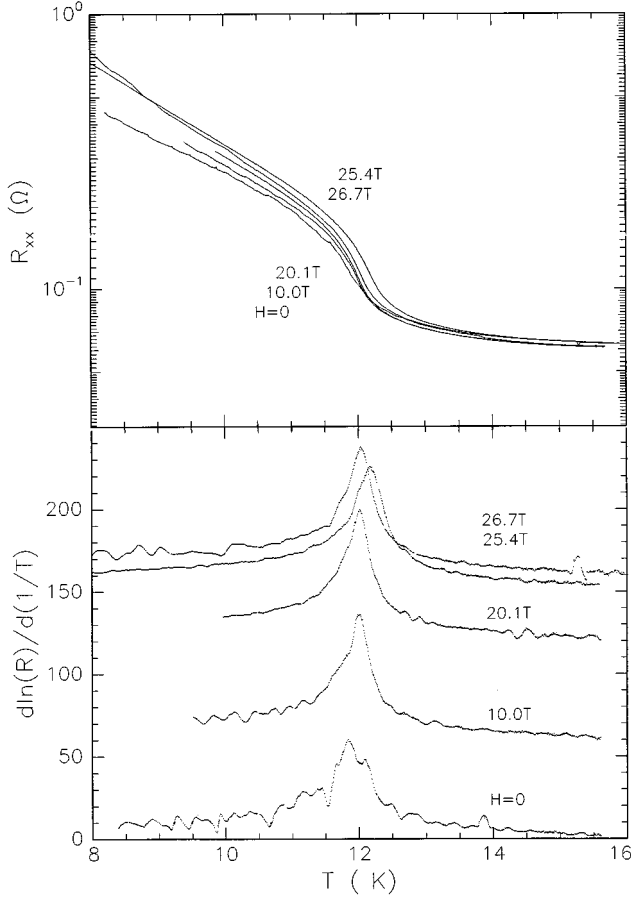


FIG. 2. (Top) temperature sweeps measuring  $R_{xx}$  in ambient pressure  $\text{PF}_6$  at constant field along the **a** axis as indicated. (Bottom) logarithmic derivatives of the data above (offsets are proportional to field). There is no field dependence to the transition temperature when the field is in the **a** direction (5/6/94, sample 2).

dicts some authors<sup>10,11</sup> who observe a small temperature dependence for fields along the **a** direction in  $\text{PF}_6$  and in  $\text{AsF}_6$ . Their experiments measure magnetic susceptibility along the **a** axis to fields of 5 T and use a sharp feature in the temperature sweeps as an indicator of  $T_{\text{SDW}}$ . It is not clear that this feature coincides with the actual phase transition, and so the calculated temperature dependence (which is quite large  $\sim 0.2$  K/T) will reflect this. Because, too, we have measured samples to much higher fields, any temperature dependence would have become apparent.

Temperature sweeps of  $R_{xx}$  were also conducted with the field in the **c** direction (Fig. 4). The character of these data is different from that when the field was oriented in the conducting plane. There is a large magnetoresistance when the field is along **c**, both above and below  $T_{\text{SDW}}$ . Even from this figure it is clear that the transition is shifted toward higher temperature as the field is increased. Derivatives of these traces are also shown in Fig. 4, and the peaks in the derivative are plotted vs field in Fig. 5. The observed shift in critical temperature with field is in agreement with thermodynamic measurements,<sup>12</sup> and there is good agreement with an  $H^2$  dependence for the transition temperature. Previous studies<sup>13</sup> have failed to observe a shift in  $T_{\text{SDW}}$  in fields to 8 T, where the effect would be  $\sim 0.1$  K according to our results. The sensitivity of the experiment may not have been able to detect this effect.

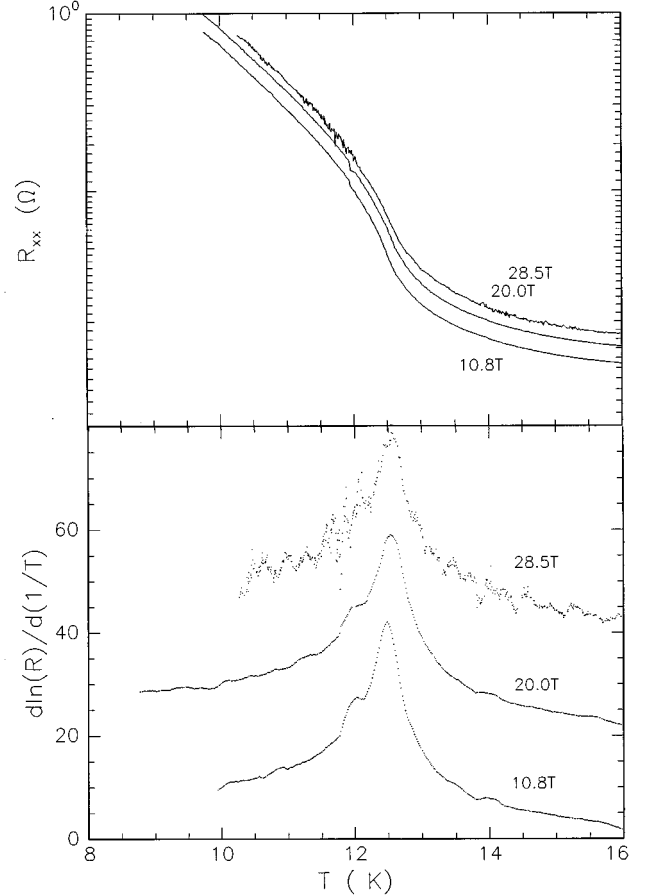


FIG. 3. (Top) temperature sweeps measuring  $R_{xx}$  in ambient pressure  $\text{PF}_6$  at constant field along the **b** axis as indicated. (Bottom) logarithmic derivatives of the data above (offsets are proportional to field). There is no field dependence to the transition temperature when the field is in the **b** direction (5/5/94, sample 1).

From the observed curvature of the field dependence and the zero-field transition temperature, we can determine several important parameters for the SDW transition. Using the curvature and Eq. (3), we measure  $f(\beta)/t_b'^* = 0.0016/\text{K}$  with zero applied pressure. The curvature function  $f(\beta)/t_b'^*$  depends separately on the degree of imperfect nesting ( $\beta$ ) and the critical imperfect nesting ( $t_b'^*$ ). However, we also observe the transition temperature as 12.1 K which separately constrains  $\beta$  and  $t_b'^*$ . From these two factors we arrive at a self-consistent solution of  $t_b' = 4.5 \pm 0.3$  K,  $t_b'^* = 11.3 \pm 0.2$  K, and  $T_{\text{SDW}} = 12.1 \pm 0.1$  K for  $\text{PF}_6$  at zero applied pressure within the theoretical formulation of Ref. 4. Montambaux states that the estimated value of  $t_b'$  is between 5 and 10 K. Our measurement is on the lower end of this range, but is not in substantial disagreement.

The analytic form of a quadratic variation with field of  $T_{\text{SDW}}$  [Eq. (3)] is valid only for the region  $\omega_c < t_b'$ . When  $\omega_c \gg t_b'$  the field dependence of the critical temperature is expected to saturate to its value in the absence of imperfect nesting, in zero applied field. Our measurements to 28.5 T do not show a saturation in the  $H^2$  behavior of  $T_{\text{SDW}}$ . For a field of 30 T,  $\omega_c \sim 27$  K, and so we are perhaps just approaching the saturation regime with the fields achievable at the Francis Bitter National Magnet Laboratory.

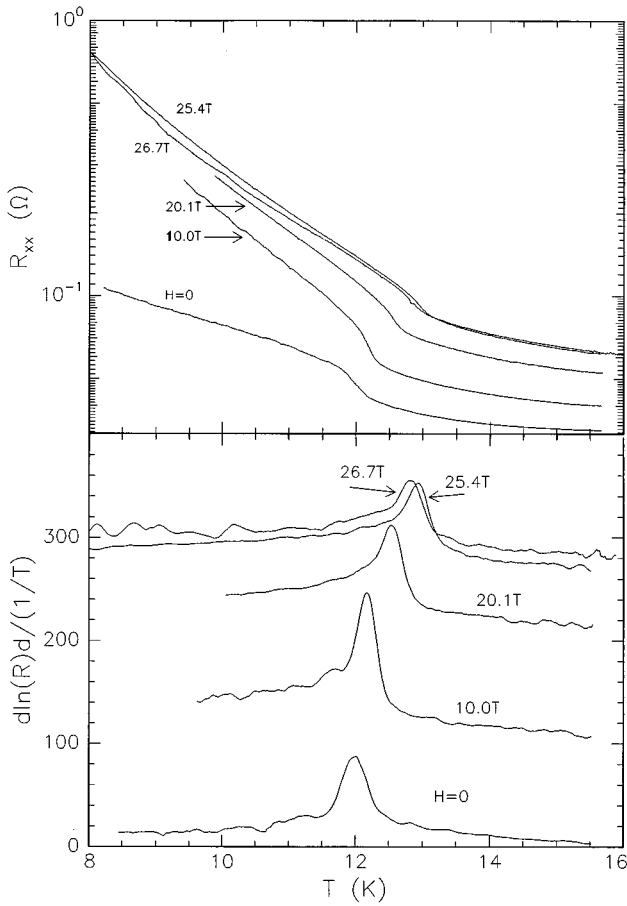


FIG. 4. (Top) temperature sweeps measuring  $R_{xx}$  in ambient pressure  $\text{PF}_6$  at constant field along the  $c$  axis as indicated. (Bottom) logarithmic derivatives of the data above. The offsets are proportional to field; consequently one can observe the  $H^2$  field dependence of the transition temperature (5/6/94, sample 1).

### B. $T_{\text{SDW}}$ under hydrostatic pressure

We have also made measurements of  $R_{zz}$  in  $\text{PF}_6$  under hydrostatic pressure (Fig. 6). The field dependence of the

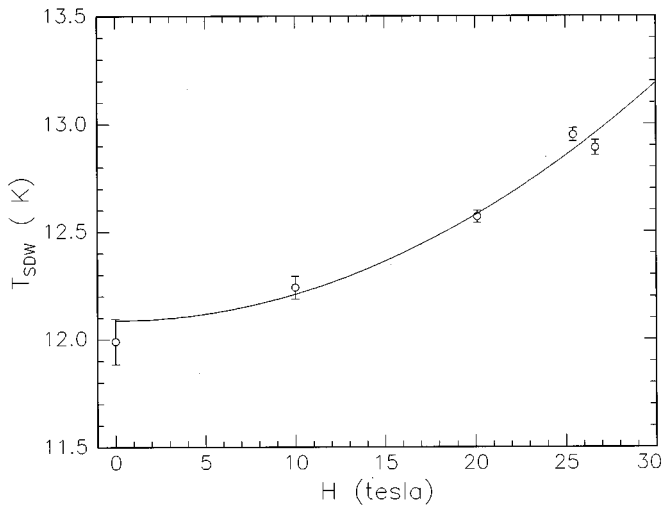


FIG. 5. Critical temperatures determined from Fig. 4. The fit is to  $T_{\text{SDW}} = 12.1 + 0.00123H^2$ .

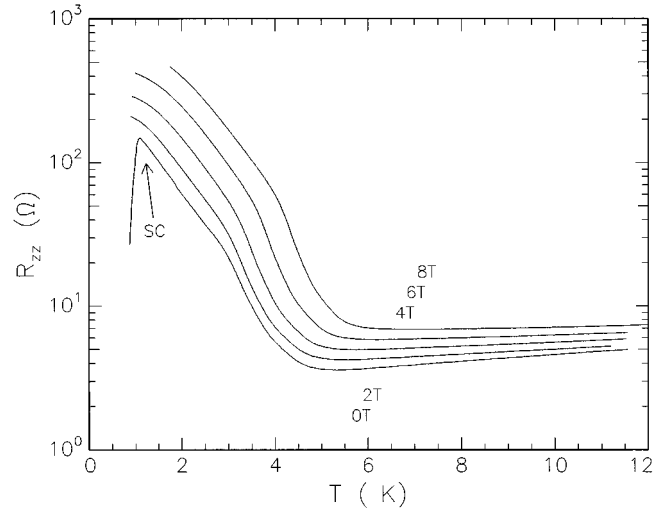


FIG. 6. Measurements of  $R_{zz}$  in  $\text{PF}_6$  at 5.2 kbar during temperature sweeps at constant field along the  $c$  axis. This sample is close enough to the critical pressure that a superconducting transition is observed in the zero field trace a  $T \sim 1$  K (6/6/94).

transition temperature is much larger when the pressure is near critical than at ambient pressure. This is expected because the field is more important in stabilizing the SDW when the sample is near the critical pressure. From the fit to the field dependence (Fig. 7) we measure  $f(\beta)/t_b'^* = 0.022/\text{K}at$   $5.2 \pm 0.2$  kbar. Using the value of  $t_b'^*$  determined from the ambient pressure data we obtain  $t_b' = 11.0 \pm 0.3$  K with  $T_{\text{SDW}} = 3.3 \pm 0.1$  K. Considering that the agreement of all three parameters is somewhat subtle, it is reassuring that the value for the critical imperfect nesting determined from  $p=0$  data agrees well with the data obtained at higher pressures. We made measurements on one additional sample under pressure, and the results using the measured  $T_{\text{SDW}}$  ( $\sim 7$  K) and curvature agreed well with the present results. Unfortunately we were unable to obtain an accurate pressure on this sample, and so it is not included

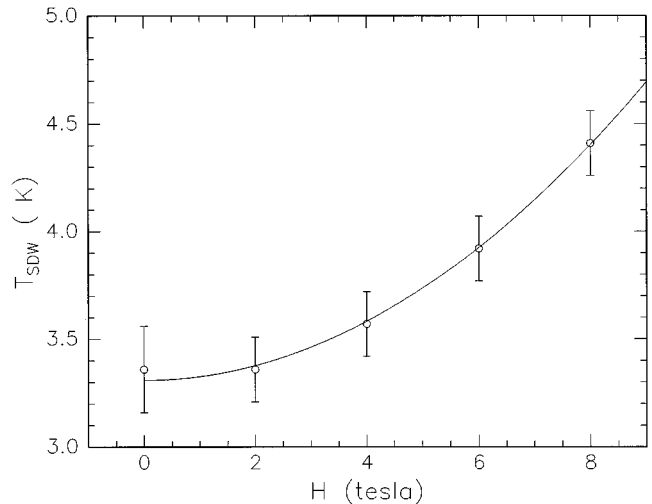


FIG. 7. Critical temperatures measured on  $\text{PF}_6$  under 5.2 kbar of pressure. The field is oriented along the  $c$  axis. The fit is to  $T_{\text{SDW}} = 3.3 + 0.0171H^2$ .

with these data. Kwak *et al.*<sup>14</sup> have measured this curvature for samples at 6.3 kbar as  $f(\beta)/t_b'^* = 0.024 - 0.031/\text{K}$  (the critical pressure has been measured as 6.5 kbar in Ref. 15). Using  $\beta=1$  and our value of  $t_b'^* = 11.3 \text{ K}$ , the curvature at the critical pressure should be  $0.027/\text{K}$ , which is consistent with the results in Ref. 14.

## V. SUMMARY

The theory of Montambaux provides a consistent theoretical framework in which to interpret the SDW transitions in  $\text{PF}_6$ . It accounts for the field dependence and the pressure dependence of the transition in terms of one parameter: the deviation from perfect nesting.

We have measured the pressure and field dependence of the SDW transition temperature. We find that at ambient pressure the transition occurs at  $12.1 \pm 0.1 \text{ K}$ . From this and the **c** axis field dependence of  $T_{\text{SDW}}$ , we have determined the critical imperfect nesting bandwidth as  $t_b'^* = 11.3 \pm 0.2 \text{ K}$  with the imperfect nesting bandwidth as  $t_b' = 4.5 \pm 0.3 \text{ K}$ .

The measurements are consistent with previous results. We have also made observations of the SDW transition for fields along the **a** and **b** axes and find no field dependence to  $T_{\text{SDW}}$ . At higher pressures the critical temperature is reduced; at  $5.2 \pm 0.2 \text{ kbar}$ ,  $T_{\text{SDW}}$  is  $3.3 \pm 0.1 \text{ K}$ . We find a consistent solution for the imperfect nesting bandwidth for the pressurized sample using the same critical value as at ambient pressure data and  $t_b' = 11.0 \pm 0.3 \text{ K}$ . At pressures near the critical pressure, the SDW and superconductivity compete. As the temperature is lowered on the 5.2 kbar sample it becomes superconducting  $\sim 1 \text{ K}$ . These measurements are consistent with other observations of the field dependence of  $T_{\text{SDW}}$  near the critical pressure.

## ACKNOWLEDGMENTS

We would like to thank the Francis Bitter National Magnet Laboratory for their help in conducting these experiments. This research was supported by the National Science Foundation through Grant No. NSFDMR92-04581.

\*Present address: University of Colorado at Boulder, Physics Department, Condensed Matter Laboratory, Campus Box 390, Boulder, CO, 80309; dannerg@spot.colorado.edu

<sup>1</sup>R.E. Peierls, *Quantum Theory of Solids* (Oxford University Press, London, 1953), p. 108.

<sup>2</sup>For a review, see T. Isiguro and K. Yamaji, *Organic Superconductors* (Springer-Verlag, Berlin, 1990); for more recent references see G. Danner *et al.*, *Physica* **B201**, 442 (1994); *Synth. Met.* **70**, 731 (1995).

<sup>3</sup>K. Yamaji, *J. Phys. Soc. Jpn.* **51**, 2787 (1982).

<sup>4</sup>G. Montambaux, *Phys. Rev. B* **38**, 4788 (1988).

<sup>5</sup>B. Horowitz, H. Gutfreund, and M. Weger, *Phys. Rev. B* **12**, 3174 (1975); P.M. Chaikin, P. Pincus, and G. Beni, *J. Phys. C* **8**, L65 (1975).

<sup>6</sup>T. Takahashi *et al.*, *J. Phys. Soc. Jpn.* **55**, 1364 (1986).

<sup>7</sup>W. Kang, Ph.D. thesis, Princeton University, 1992.

<sup>8</sup>X. Chen, A.S. Perel, J.S. Brooks, R.P. Guertin, and D.G. Hinks, *J. Appl. Phys.* **73**, 1886 (1993).

<sup>9</sup>M.J. Clark and T.F. Smith, *J. Low Temp. Phys.* **32**, 495 (1978).

<sup>10</sup>K. Mortensen, Y. Tomkiewicz, T.D. Schultz, and E.M. Engler, *Phys. Rev. Lett.* **46**, 1234 (1981).

<sup>11</sup>K. Mortensen, Y. Tomkiewicz, and K. Bechgaard, *Phys. Rev. B* **25**, 3319 (1982).

<sup>12</sup>J. Coroneus, B. Alavi, and S.E. Brown, *Phys. Rev. Lett.* **70**, 2332 (1993).

<sup>13</sup>P.M. Chaikin, P. Haen, E.M. Engler, and R.L. Greene, *Phys. Rev. B* **24**, 7155 (1981).

<sup>14</sup>J.F. Kwak, J.E. Schirber, P.M. Chaikin, J.M. Williams, and H. Wang, *Mol. Cryst. Liq. Cryst.* **125**, 375 (1985).

<sup>15</sup>D. Jerome, *Mol. Cryst. Liq. Cryst.* **79**, 155 (1982).